ARCHIVES OF ELECTRICAL ENGINEERING VOL. 68(2), pp. 227–235 (2019)

DOI 10.24425/aee.2019.128264

Voltage modelling in ignition coil using magnetic coupling of fractional order

SEBASTIAN RÓŻOWICZ

Kielce University of Technology, Poland
e-mail: s.rozowicz@tu.kielce.pl

(Received: 01.10.2018, revised: 20.12.2018)

Abstract: The paper discusses the modelling of magnetic coupling in ignition coils by fractional differential equations. The use of fractional-order coupling allows us to consider the losses caused by the non-linearity of the ferromagnetic core of the ignition coil and obtain the waveform of the ignition coil's secondary voltage closest to the values obtained experimentally.

Key words: ignition system, fractional-order magnetic coupling, CFE method, Oustaloup method

1. Introduction

It is difficult to characterize the dynamics of the modern ignition system, as the analytical results and digital simulation differ from the experimental data. The mathematical model of the ignition system is represented by differential non-linear equations (in particular case as a linear system). The secondary voltage produced in the secondary winding of the ignition coil has a significant influence on the combustion process of the air-fuel mixture. A proper identification of the shape and parameters of the secondary voltage allows us to effectively model the spark discharge, which largely determines the combustion process of the fuel-air mixture.

The ability to model and later control the secondary voltage allows us to reduce the toxicity of fumes and to protect the natural environment by controlling the spark discharge energy. The results of experimental measurements differ significantly from digital simulations using classical differential equations describing the voltage waveform in the dynamics of ignition systems. Therefore, the author has attempted to model the system's response replacing the classical system of differential equations with fractional calculus. The modelling solution [1–4] for different fractional orders of the equation was selected so as to match as closely as possible the waveforms

obtained experimentally. To solve the fractional differential equation modelling the spark discharge system, the solution was approximated by continued fraction expansion (CFE) and the Oustaloup methods.

2. Model of the ignition system

One of the most important physical phenomena in ignition coils is magnetic coupling. According to the principle of commutation, the current cannot change abruptly when the voltage is applied to the coil. On the other hand, turning off the voltage, which is equivalent to stopping the current in the coil, contradicts this principle. Theoretically, the voltage on the coil during the interruption of the current is equal to the Dirac impulse as for

$$i(t) = I_0\mathbf{1}(-t), \qquad u(t) = L\frac{\mathrm{d}i}{\mathrm{d}t} \;\Rightarrow\; u(t) = -LI_0\delta(t).$$

In order to model this voltage, a fractional model was used. This allows us to transform the Dirac impulse into a form that better represents the shape and value of voltage in the real system. Consider a system of two magnetically coupled real coils (*RL* circuits) (Fig. 1).

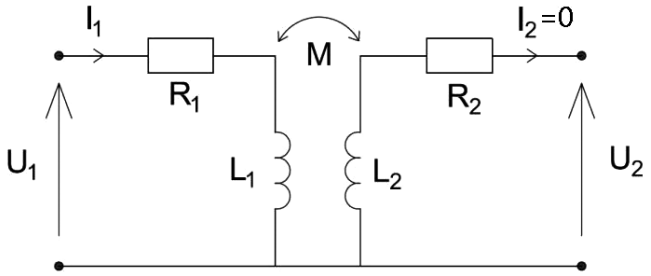

Fig. 1. Two magnetically coupled real coils (*RL* circuits). R_1 is the resistance of the primary coil, L_1 is the inductance of the primary coil, R_2 is the resistance of the secondary coil, L_2 is the inductance of the secondary coil, M is the mutual inductance

If there is no load (as in Fig. 1), we can write the system of differential equations in form (1).

$$\begin{cases} u_1 = i_1R_1 + L_1\dfrac{\mathrm{d}i_1}{\mathrm{d}t} \\ u_2 = M\dfrac{\mathrm{d}i_1}{\mathrm{d}t} \end{cases}. \tag{1}$$

(The equations are not adjoint).

Using the operator method at a zero initial condition, we get the following system of equations (1):

$$\begin{cases} U_1(s) = I_1(s)R_1 + sL_1I_1(s) \\ U_2(s) = sMI_1(s) \end{cases}. \tag{2}$$

By solving (2) we obtain voltage transforms $U_2(s)$:

$$U_2(s) = \frac{sMU_1(s)}{R_1 + sL_1}. \tag{3}$$

Assuming that the voltage $u_2(t)$ takes the form shown in the figure (Fig. 2)

$$u_1(t) = U\left[\mathbf{1}(t) - \mathbf{1}(t - t_0)\right], \tag{4}$$

where

– $\mathbf{1}(t)$ is the unit step function,

– U is the battery voltage,

– t_0 is the impulse duration

and determining its transform

$$U_1(s) = \frac{U}{s}\left(1 - e^{-st_0}\right), \tag{5}$$

we calculate the voltage transform $U_2(s)$ as follows:

$$U_2(s) = \frac{UM\left(1 - e^{-st_0}\right)}{R_1 + sL_1}. \tag{6}$$

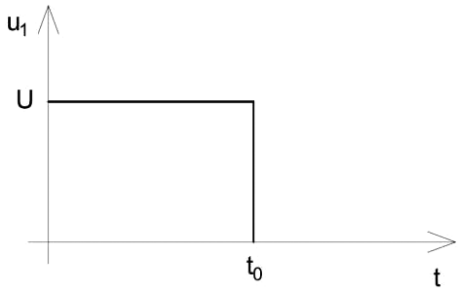

Fig. 2. Rectangular voltage function

The inverse transform, that is the voltage $u_2(t)$, is

$$u_2(t) = \frac{UM}{L_1}\left[e^{-\frac{R_1}{L_1}t}\mathbf{1}(t) - e^{-\frac{R_1}{L_1}(t-t_0)}\mathbf{1}(t - t_0)\right]. \tag{7}$$

The solution was obtained assuming the linearity of the coils without regard to losses caused by the ferromagnetic core. According to the literature, [5–7, 16, 17, 20] the omitted losses can be modelled using fractional-order derivatives.

In this case, we use the derivative only for magnetic coupling and obtain the following form of system (1):

$$\begin{cases} u_1(t) = R_1 i_1(t) + L_1 \dfrac{\mathrm{d}i_1(t)}{\mathrm{d}t} \\ u_2(t) = M_\alpha \dfrac{\mathrm{d}^\alpha i_1(t)}{\mathrm{d}t^\alpha} \end{cases}. \tag{8}$$

M_α is the mutual inductance of fractional order whose unit is expressed by the formula:

$$\left[M_\alpha = \frac{H}{s^{1-\alpha}} = \Omega s^\alpha\right].$$

The above unit results from the correctness of physical relation

$$M_\alpha \frac{\mathrm{d}^\alpha i_1}{\mathrm{d}t^\alpha},$$

where the unit of the voltage V should appear.

Since no theoretical premises concerning the value of M_α are known, it is obtained experimentally.

Consequently, in accordance with [8, 9] the system (2) is written as:

$$\begin{cases} U_1(s) = I_1(s)R_1 + sL_1I_1(s) \\ U_2(s) = s^\alpha M_\alpha I_1(s) \end{cases}. \tag{9}$$

The equations in (9) are not adjoined (as in system 1), so the current transform $I_1(s)$ is expressed by relation (2), and the voltage transform $U_2(s)$ by

$$U_2(s) = \frac{s^\alpha M_\alpha U_1(s)}{R_1 + sL_1}. \tag{10}$$

Substituting the voltage $U_1(s)$ by (5) we obtain:

$$U_2(s) = \frac{s^\alpha M_\alpha U\,(1 - e^{-st_0})}{s(R_1 + sL_1)}. \tag{11}$$

Since the fractional power s is present in Formula (11), the CFE expanding the expression $(1 + x)^\alpha$ for $0 \le \alpha \le 1$ [10] into a continued fraction is used to determine the inverse transform.

In the CFE fractional power s can be represented as the quotient of the polynomials of the variable s and the order of the derivative α. Here the variables appear as integer exponents [11, 12].

$$s^\alpha \cong \frac{N(s,\alpha)}{D(s,\alpha)} = \frac{\sum_{k=0}^{A} P_{Ak}(\alpha)s^{A-k}}{\sum_{k=0}^{A} Q_{Ak}(\alpha)s^{A-k}}, \tag{12}$$

where A is the approximation order.

$P_{Ak}(\alpha)$, $Q_{Ak}(\alpha)$ represent the polynomials α of order A.

Assuming that approximation order $A = 5$, the polynomials have the following form:

$$\begin{aligned}
P_{50}(\alpha) &= Q_{55}(\alpha) = -\alpha^5 - 15\alpha^4 - 85\alpha^3 - 225\alpha^2 - 274\alpha - 120, \\
P_{51}(\alpha) &= Q_{54}(\alpha) = 5\alpha^5 + 45\alpha^4 + 55\alpha^3 - 1\,005\alpha^2 - 3\,250\alpha - 3\,000, \\
P_{52}(\alpha) &= Q_{53}(\alpha) = 10\alpha^5 - 30\alpha^4 - 410\alpha^3 + 1\,230\alpha^2 + 4\,000\alpha - 12\,000, \\
P_{53}(\alpha) &= Q_{52}(\alpha) = -10\alpha^5 - 30\alpha^4 + 410\alpha^3 + 1\,230\alpha^2 - 4\,000\alpha - 12\,000, \\
P_{54}(\alpha) &= Q_{51}(\alpha) = -5\alpha^5 + 45\alpha^4 - 5\alpha^3 - 1\,005\alpha^2 + 3\,250\alpha - 3\,000, \\
P_{55}(\alpha) &= Q_{50}(\alpha) = \alpha^5 - 15\alpha^4 + 85\alpha^3 - 225\alpha^2 + 274\alpha - 120.
\end{aligned} \tag{13}$$

In [18] it is shown that the approximation of the $A = 5$ order gives a relatively highest accuracy for the fifth-degree polynomials. Increasing the approximation order at the cost of the increased number of terms only slightly improves the accuracy.

Thus the voltage transform at the output of the system is written as:

$$U_2(s) = \frac{UM_\alpha N(s,\alpha)\left(1 - e^{-st_0}\right)}{s(R_1 + sL_1)D(s,\alpha)}. \tag{14}$$

Since we know the value of the derivative order α, it is possible to determine an inverse transform, by using, for example, the residuum method.

The second method used to approximate the s^α factor is the expansion into the Oustaloup series where for the frequency range (ω_l, ω_h) the above factor is shown as the transfer function $H(s)$ [13–15]:

$$s^\alpha \approx H(s) = C_0 \prod_{k=-N}^{N} \frac{s + \omega'_k}{s + \omega_k}, \tag{15}$$

where:

– N is the order of approximation,

– C_0 is the gain described by the relation

$$C_0 = \left(\frac{\omega_h}{\omega_1}\right)^{-\frac{\alpha}{2}} \prod_{k=-N}^{N} \frac{\omega_k}{\omega'_k}, \tag{15a}$$

– ω'_k represents zeros of the $H(s)$ transfer function

$$\omega'_k = \omega_l \left(\frac{\omega_h}{\omega_1}\right)^{\frac{k+N+0.5(1-\alpha)}{2N+1}}, \tag{15b}$$

– ω_k represents poles of the $H(s)$ transfer function

$$\omega_k = \omega_l \left(\frac{\omega_h}{\omega_1}\right)^{\frac{k+N+0.5(1+\alpha)}{2N+1}}. \tag{15c}$$

Substituting Formula (14) according to (15):

$$N(s,\alpha) = C_0 \prod_{k=-N}^{N} \left(s + \omega'_k\right), \qquad D(s,\alpha) = C_0 \prod_{k=-N}^{N} \left(s + \omega_k\right),$$

we obtain the Oustaloup approximation of the voltage transform $u_2(t)$. Since it contains only the integer exponents of s, we can determine the inverse transform by using standard methods.

3. Laboratory experiments

The experiment consisted in recording voltage at the secondary terminals of the ignition coil. A DPO 4104 digital oscilloscope was used to record the u_2 voltage. The recorded waveform is shown in Fig. 3.

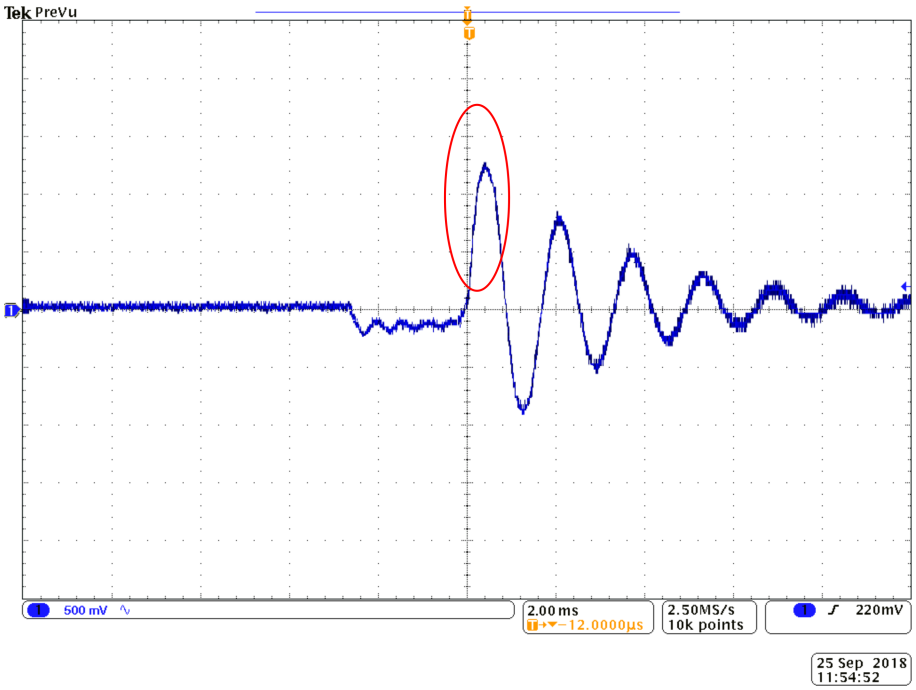

Fig. 3. Oscillogram of u_2 voltage

The time waveform of the secondary voltage $u_2(t)$ of the ignition coil induced by the magnetic coupling was recorded in the absence of spark discharge. The spark discharge on the spark plug takes place when the u_2 voltage rises (this section of the waveform is marked red in Fig. 3. In view of the above it appears that it is important to model the $u_2(t)$ voltage and the moment of ignition at the u_2 rise in this particular section of the time waveform.

4. Numerical experiments

Mathematical modelling of the $u_2(t)$ voltage consists in performing a series of numerical experiments to develop the model most accurately describing the real waveform presented in Fig. 3. The modelling was conducted for the power supply of the primary winding in the form of a unit function. For numerical experiments the following parameters of the ignition coil were used: $L_1 = 0.01$ H; $L_2 = 40$ H; $M_\alpha = 0.57\ \Omega s^\alpha$; $R_1 = 2.8\ \Omega$; $R_2 = 4\,000\ \Omega$; $U = 12$ V.

The fractional calculus was used to approximate the u_2 waveform. The derivatives were calculated using CFE and Oustaloup methods, and the simulation was conducted for α fractional-order derivatives from 1.0 to 0.7. The results for $\alpha = 0.9$ and $\alpha = 0.8$ are presented below. To assess how well the model matches the parameters of the real object, the $u_2(t)$ waveforms for classical coupling (u_k), fractional coupling calculated by CFE – (u_f), and the Oustaloup (u_O)

approximation of the fifth order at given α values were compared with the laboratory results. The first stage included the simulations at $\alpha = 0.9$.

The results in Fig. 4 show that the $u_2(t)$ waveforms determined by the Oustaloup and CFE methods are similar to the waveforms obtained by measuring the real object only for the initial phase of voltage rise (up to approx. 300 V). The next phase shows considerable differences both in the rate of the voltage rise and its maximum value. Thus the waveform matching is unsatisfactory in both cases (both in the Oustaloup and CFE methods). The further stage included the simulations at $\alpha = 0.8$. The results are shown in Fig. 5.

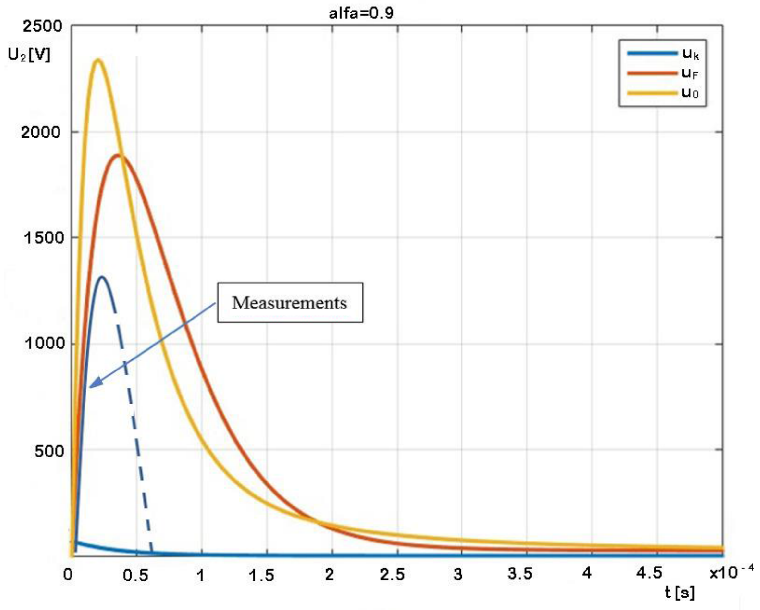

Fig. 4. The waveforms of $u_2(t)$ voltage for classical coupling (u_k) and fractional coupling calculated using CFE – (u_f) and Oustaloup (u_O) methods at $\alpha = 0.9$

For loads with fractional-order coupling, we assume that

$$M_\alpha = 0.57 \frac{H}{s^{1-\alpha}} .$$

There are no theoretical premises concerning the value of a fractional-order coupling coefficient so, we choose its unit and α value on the basis of experimental results.

The results of the u_2 voltage simulations for $\alpha = 0.8$ obtained using the Oustaloup method [19] confirm good matching of the waveforms and can serve as a model of the u_2 voltage resulting from the fractional coupling. In all simulations for α from 1.0 to 0.7, a better waveform matching was obtained for the fractional method than for the classical one (the results of the classical method are presented in [2, 11]).

The results of the tests clearly indicate that magnetic coupling is of fractional order.

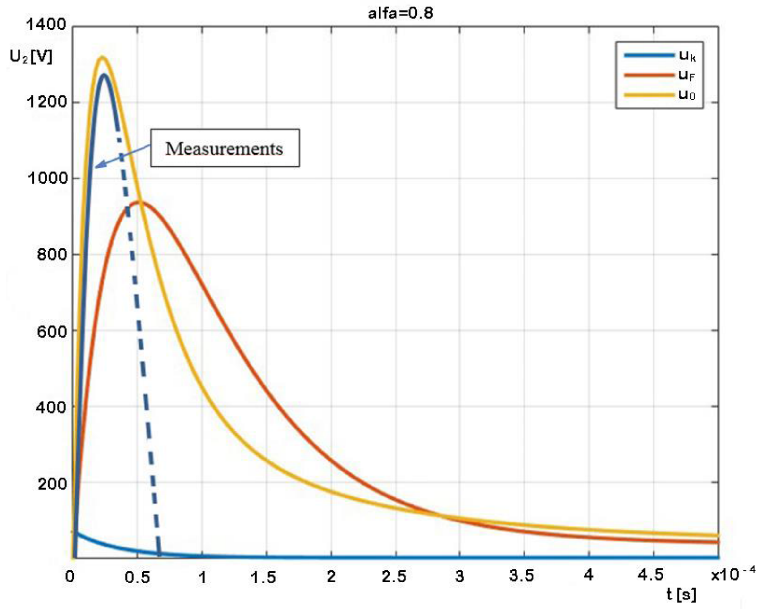

Fig. 5. The waveforms of $u_2(t)$ voltage for classical coupling (u_k) and fractional coupling calculated using CFE – (u_f) and Oustaloup (u_O) methods at $\alpha = 0.8$

5. Conclusions

As seen in Figs. 4 and 5, the secondary voltage waveform modelled (until the ignition starts) by the fractional-order coupling matches the empirical waveform, (the best results were obtained for $\alpha = 0.8$ using the Oustaloup method). The use of the fractional-order coupling takes into account the losses caused by the non-linearity of the ferromagnetic core of the ignition coil, which has not been considered in earlier models. We can conclude that the use of the correct α order allows for the consideration of losses resulting from the coupling, non-linearity and other empirical parameters of the ignition coil.

References

[1] Herner A., Herner A., Riehl H.J., *Electrotechnics and Electronics in Motor Vehicles* (in Polish) (2003).

[2] Różowicz S., Tofil S., *The influence of impurities on the operation of selected fuel ignition systems in combustion engines*, Archives of Electrical Engineering, vol. 65, no. 2, pp. 349–360 (2016).

[3] Stone C., Brown A., Beckwith P., *Cycle-by-cycle variations in spark ignition engine combustion – part II: modelling of flame kernel displacements as a cause of cycle-by-cycle variations*, SAE paper 960613 (1996).

[4] Zawadzki A., Różowicz S., *Application of input – state of the system transformation for linearization of some nonlinear generators*, International Journal of Control, Automation and Systems, vol. 13, no. 3, pp. 1–8 (2015), DOI: 10.1007/s12555-014-0026-3.

[5] Schäfer I., Krüger K., *Modelling of lossy coil using fractional derivatives*, Journal of Physics D: Applied Physics, vol. 41, pp. 1–8 (2008).

[6] Vorperian V., *A fractal model of anomalous losses in ferromagnetic materials*, 23rd Annual IEEE Power Electronics Specialists Conference, MAG-28, pp. 1277–1283 (1992).

[7] Zawadzki A., Różowicz S., *Application of input-state of the system transformation for linearization of selected electrical circuits*, Journal of Electrical Engineering (Elektrotechnicky Casopis), vol. 67, no. 3, pp. 199–205 (2016).

[8] Ostalczyk P., *Elements of Fractional Calculus*, Publishing House of Łódź University of Technolgy (in Polish) (2008).

[9] Kaczorek T., Rogowski K., *Fractional Linear Systems and Electrical Circuits*, Białystok University of Technology (2014).

[10] Khovanskii A.N., *The application of continued fractions and their generalizations to problems in approximation theory*, Noordhoff, The Netherlands (1963).

[11] Różowicz S., *Influence of fuel impurities on the consumption of electrodes in spark plugs*, Open Physics, vol. 16, iss. 1, pp. 57–62 (2018).

[12] Krishna B.T., *Studies on fractional order differentiators and integrators: A survey*, Signal Processing 91, pp. 386–426 (2011).

[13] Oustaloup A., Levron F., Mathieu B., Nanot F.M., *Frequency-band complex no integer differentiator: characterization and synthesis*, EEE Transactions on Circuits and Systems I: Fundamental Theory and Applications, vol. 47, iss. 1, pp. 25–39 (2000).

[14] Różowicz S., *The effect of different ignition cables on spark plug durability*, Przegląd Elektrotechniczny, vol. 94, iss. 4, pp. 191–195 (2018).

[15] Marushak Y., Kopchak B., *Analysis of Models of Fractional Integration and Differentiation* (in Polish), Elektrotechnika 34, vol. 2, pp. 213–222 (2015).

[16] Tarimer J.A., Arslan S., Guwen M.E., *Investigation for Losses of M19 and Amorphous Core Materials Asynchronous Motor by Finite Elements Methods*, Elektronika Ir Elektrotechnika, vol. 18, no. 9, pp. 15–18 (2012), DOI: http://dx.doi.org/10.5755/j01.eee.18.9.2797.

[17] Tarimer J.A., Guwen ME., Arslan S., *Computer Aided Design of An Electromagnetic Ignition Coil For High Speed Benzene Engines*, Przegląd Elektrotechniczny, vol. 87, pp. 230–236 (2011), http://pe.org.pl/articles/2011/2/51.

[18] Zawadzki A., Włodarczyk M., *CFE method-utility analysis of the approximation of reverse Laplace transform of fractional order*, IC SPETO, pp. 45–46 (2015).

[19] Baranowski J., Bauer W., Zagórowska M., Dziwiński T., Piątek P., *Time-domain Oustaloup approximation*, Conference paper, Methods and Models in Automation and Robotics (MMAR), 20th International Conference on Międzyzdroje, Poland (2015), DOI: 10.1109/MMAR.2015.7283857.

[20] Latawiec K.J., Stanisławski R., Łukaniszyn M., Czuwara W., Rydel M., *Fractional-order modeling of electric circuits: modern empiricism vs. classical science*, Progress in Applied Electrical Engineering (PAEE) (2017), 10.1109/PAEE.2017.8008998.